Catalytic modification of pyrolysis products of nitrogen-containing polymers over Y zeolites

János Bozi* and Marianne Blazsó

Received 29th May 2009, Accepted 10th July 2009
First published as an Advance Article on the web 30th July 2009
DOI: 10.1039/b913894n

Pyrolysis products of nitrogen-containing polymers have been transformed at 500 °C over NaY and ultra stable HY (HUSY) zeolite on-line and analysed by gas chromatography/mass spectrometry. HUSY was found to be an effective catalyst converting nitrogen-containing compounds into a series of well-defined aromatic hydrocarbons. Almost all nitrogen-content of the pyrolysis oils including amines, amides and nitriles have been successfully eliminated over HUSY; only traces of aliphatic nitriles in the range of 3–8 carbon atoms still remained in some of the pyrolysis oils. The uniform composition of the converted pyrolysis oil offers the possibility to gain pure aromatic feedstock from plastics waste. NaY proved to be an effective catalyst for cracking the heavy oil components of polymer pyrolysates to gases and to compounds of gasoline volatility, nevertheless it was not active for denitrogenation. Thermal treatment of deactivated zeolite has been carried out to study catalysts regeneration. By means of regeneration at 500 °C in air flow for 8 hours the activity of NaY has been completely recovered, while in the case of HUSY a slight decrease of activity was observed after the same treatment.

Introduction

The amount of disposed waste electronic and electric equipment (WEEE) is increasing from year to year. Therefore WEEE management has become a key issue in many countries recently. However, for recycling multi-component polymer waste—such as the plastics in WEEE and automotive plastic shredder—scientists have to surmount several obstacles. Since these plastics mixtures contain various kinds of oxygen-, nitrogen- and halogen-containing polymers, fire retardants and other additives their recycling is a complex and vast job. Therefore those alternative technologies are preferred that find solution to avoid environmental contamination related to halogen- and nitrogen-containing organic compounds.

As a prosperous waste management technique pyrolysis has great importance in the field of plastics recycling as well. Energy recovery by producing fuel, monomer and oligomer recovery, feedstock recycling and production of valuable substances from polymers by pyrolysis has been the subject of several research and development works in the last decade.[1] For the detailed study of the pyrolysis processes and the identification of pyrolysis products thermal analysis and pyrolysis-gas chromatography/mass spectrometry (Py-GC/MS) are more often applied. Thermal decomposition mechanism and product analysis of polymers that are components of electronic and electric equipments have been extensively studied already for more than twenty years.[2–4] Product analysis revealed the presence of hazardous and environmentally unacceptable compounds[5–6] and initiated research on changing pyrolysis products either by catalytic pyrolysis[7] or by catalytic modification of pyrolysis products.

Catalytic hydrodenitrogenation and hydrodehalogenation are both at laboratory scale and industrially used processes for reducing the level of nitrogen and halogen content of organic materials. The most often used catalyst are noble and transition metal catalysts on alumina, silica and carbon supports, moreover a number of studies have focused on catalyst modification and development[8–9] for reducing components of pollution potential in pyrolysis oil.

Sarbak and Lewandowski revealed that NiMo catalysts supported on faujasite (X and Y) type zeolites have greater hydrodenitrogenation activity than the unmodified zeolites.[8]

Ferdous *et al.* prepared and tested a series of NiMo/Al_2O_3 promoted with boron and phosphorus for hydrodenitrogenation and hydrodesulfurization as well.[9]

For dehalogenation and denitrogenation oxides, composite catalysts[10], mezoporous materials (*e.g.* MCM-41) and various zeolites have also been often applied.[11–13] Although zeolites have a number of advantageous properties, such as well-defined structure, thermal stability (A, X and Y are stable at least to 700 °C), low price and commercial availability, their usage has limits because of low resistance to mineral acids and alkalis. Additionally, coke formation on zeolite surface is the most frequent cause of catalyst deactivation. Therefore characterization of coke, coked catalysts and its regeneration also may give valuable information[14–16] about the effectiveness of these catalysts in polymer recycling.

The aim of this study was to examine the effect of zeolites on the thermal catalytic conversion of pyrolysis gases and oils

---

Department of Environmental Chemistry, Institute of Materials and Environmental Chemistry, Chemical Research Center, Hungarian Academy of Sciences, P.O. Box 17, H-1525, Budapest, Hungary. E-mail: bozij@chemres.hu; Tel: +36 1 438 1100/473

of nitrogen-containing polymers that are typical components of WEEE and automotives plastic shredder. We have also tested catalyst regeneration studying structural and activity changes.

2.0 Results and discussion

The Y type zeolites studied (NaY and HUSY) have significant effect on the pyrolysates of polyamides. Both have strong catalytic cracking activity, however the characteristic compounds of modified pyrolysis oils are different in the cases of NaY and HUSY.

2.1 Pyrolysis products of polyamides

GC/MS analysis of polyamide pyrolysis oils revealed a wide range of N-containing compounds. Amines, amides and nitriles are found in these pyrolysates beside CO_2, unsaturated and cyclic hydrocarbons demonstrated in Fig. 1–3a.

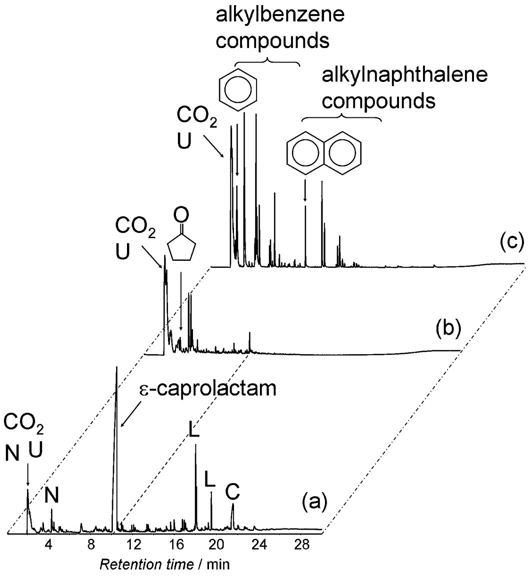

Fig. 1 Pyrolysis-gas chromatogram of PA-6 at 500 °C (a), the chromatogram of the pyrolysate converted over NaY (b) and over HUSY zeolite (c). C, cyclic amides; L, acyclic amides; N, nitriles; U, unsaturated and/or cyclic hydrocarbons.

The pyrogram of polyamide-6 (PA-6) (Fig. 1a) shows that ε-caprolactam is the most important thermal decomposition product; moreover characteristic polyamide pyrolysis oil components (N-containing and unsaturated hydrocarbons) are also present.

It is clear from Fig. 2a that thermal decomposition of polyamide-6,6 (PA-6,6) is more complex. Most of the products are N-containing; furthermore CO_2, cyclopentanone and many unsaturated and/or cyclic hydrocarbons of low molecular mass are also present in the pyrolysate. Identification of pyrolysis oil components and thermal decomposition mechanism of PA-6,6 have been published earlier.[17]

The chromatogram in Fig. 3a shows that the number and amount of unsaturated hydrocarbons are higher in the pyrolysate of polyamide-12 (PA-12) than in those of PA-6 and PA-6,6. The hydrocarbon segment of ten carbon atoms between the amide groups in PA-12 polymer chain is fragmented to a series of alkenes, alkylamines and alkylnitriles.

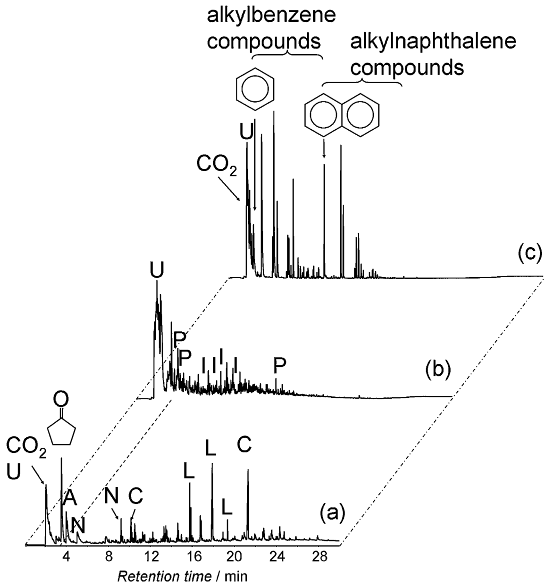

Fig. 2 Pyrolysis-gas chromatogram of PA-6,6 at 500 °C (a), the chromatogram of the pyrolysate converted over NaY (b) and over HUSY zeolite (c). A, amines; C, cyclic amides; I, indane and/or indene compounds; L, acyclic amides; N, nitriles; P, heterocyclic (N-containing) aromatic compounds; U, unsaturated and/or cyclic hydrocarbons.

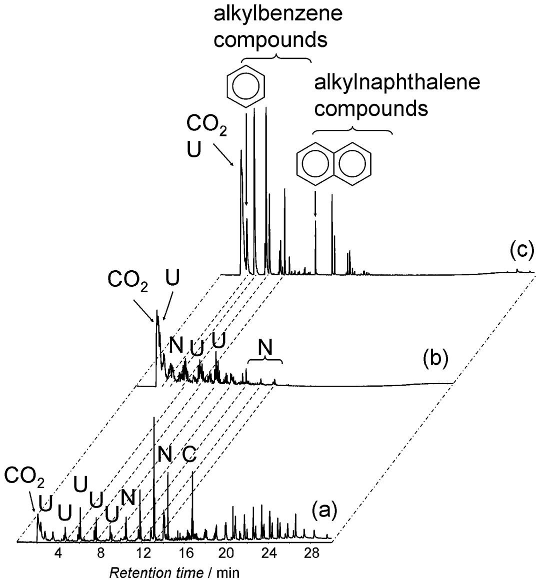

Fig. 3 Pyrolysis-gas chromatogram of PA-12 at 500 °C (a), the chromatogram of the pyrolysate converted over NaY (b) and over HUSY zeolite (c). C, cyclic amides; N, nitriles; U, unsaturated and/or cyclic hydrocarbons.

In addition to the experiments with Y zeolites catalytic transformation of PA-6,6 thermal decomposition products was also performed over Na-β and H-β zeolites. Although β zeolites have a framework structure different from that of Y type zeolites the results of conversion were very similar to those that we obtained over NaY and HUSY respectively. Therefore we assume that the catalytic effect of the zeolites is related mainly to the character of the cations.

2.1.1 Conversion over NaY. The (b) pyrograms in Fig. 1–3 show that several pyrolysis products of polyamides either disappear or notably diminish over NaY. Heavy oil components of polymer pyrolysates are cracked to gases and to compounds of gasoline volatility, therefore no peaks occur after 15 minutes retention time. The first unresolved peaks of retention time between 2 to 3 minutes cover mostly gases (CO_2, NH_3, H_2O), unsaturated olefins of 2–6 carbon atoms, nitriles and amines. Wide range of aromatics is also present with low intensity. Long chain amides and amines are converted to aromatic, alkylaromatic and cyclic N-containing compounds—such as pyridine, pyrrol, tetrahydroquinoline and their alkyl derivatives; moreover small molecular mass nitriles still remain in the pyrolysate.

2.1.2 Conversion over HUSY. The main volatile compounds of the converted pyrolysis products of polyamides over HUSY are mostly aromatics. In particular toluene, xylenes, naphthalene and methylnaphthalenes occur, but several other alkylbenzene and alkylnaphthalene compounds are present as well in the (c) chromatograms displayed in Fig. 1–3. Both coke formation on the zeolite and the multitude of aromatics in the pyrograms are generally observed in the experiments with HUSY. Nitriles in the range of 3–6 carbon atoms are the only N-containing compounds detected in the pyrolysis oil of PA-6 and PA-6,6. Among the modified pyrolysis products of PA-12 there are nitriles up to eight carbon atoms; however their amount rapidly decreases with increasing molecular mass.

2.2 Pyrolysis products of polyacrylonitrile (PAN) and styrene-acrylonitrile *co*-polymers

The total ion chromatogram of PAN pyrolysis products are shown in Fig. 4 together with those of the catalytically modified pyrolysates. The pyrolysis oil of PAN contains only nitrile compounds (Fig. 4a) including HCN, monomer, dimer, trimer and aromatic nitriles such as benzonitrile.

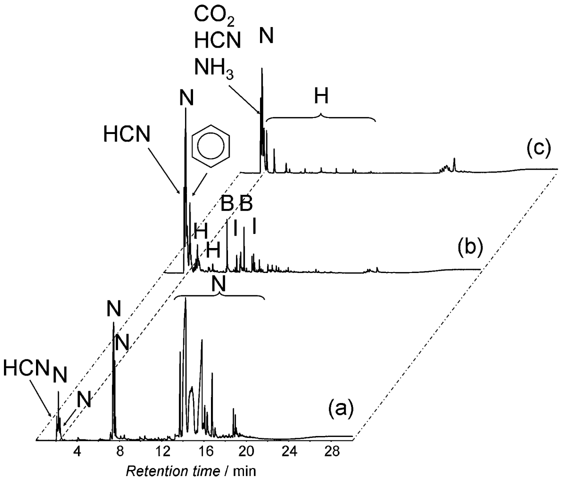

Fig. 4 Pyrolysis-gas chromatogram of PAN at 500 °C (a), the chromatogram of the pyrolysate converted over NaY (b) and over HUSY zeolite (c). B, CN-containing aromatic (mainly benzonitrile or benzyl nitrile) compounds; H, aromatic hydrocarbons; I, indane and/or indene compounds; N, nitriles.

Pyrolytic decomposition of poly(acrylonitrile-*co*-butadiene-*co*-styrene) (ABS) and poly(styrene-*co*-acrylonitrile) (SAN) is analogous, therefore the pyrograms of Fig. 5a and Fig. 6a are hardly distinguishable, and the corresponding modified pyrolysates are similar as well. The only difference is that small peaks of butadiene and related compounds are observable in the pyrogram of ABS. For ABS and SAN the main components of the pyrolysis oils are monomers, moreover dimers and trimers composed of styrene and acrylonitrile.

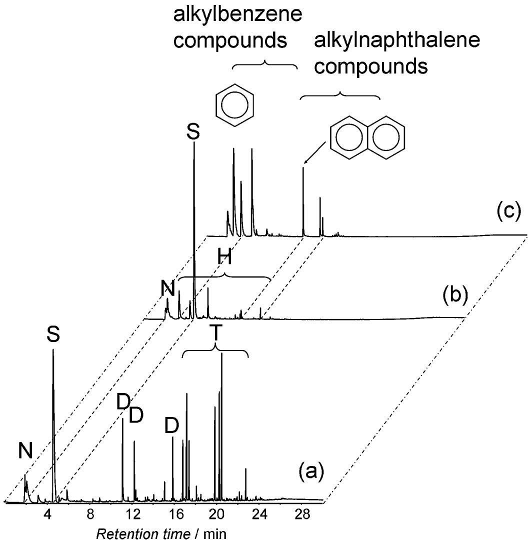

Fig. 5 Pyrolysis-gas chromatogram of ABS at 500 °C (a), the chromatogram of the pyrolysate converted over NaY (b) and over HUSY zeolite (c). D, dimers; H, aromatic hydrocarbons; N, nitriles; S, styrene; T, trimers.

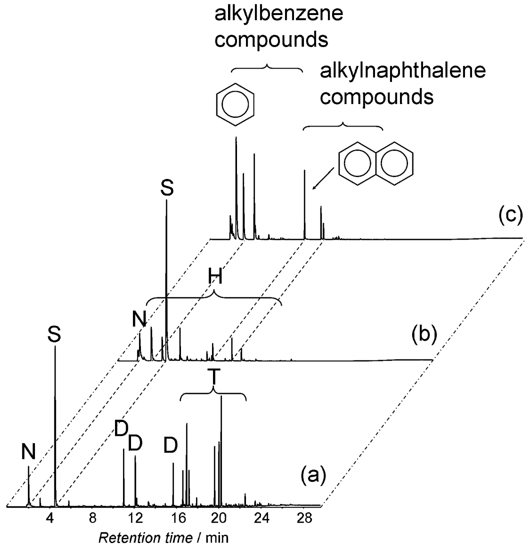

Fig. 6 Pyrolysis-gas chromatogram of SAN at 500 °C (a), the chromatogram of the pyrolysate converted over NaY (b) and over HUSY zeolite (c). D, dimers; H, aromatic hydrocarbons; N, nitriles; S, styrene; T, trimers.

2.2.1 Conversion over NaY. When NaY was used as a catalyst to transform PAN pyrolysis oil, the quantity of low

Table 1 GC-MS selected ion peak areas [(counts/mg polymer) ×10^{-7}] of small molecular mass nitriles in (a) and (c) chromatograms of PAN (Fig. 4)

Compounds and selected ions (m/z)	*Retention time*/min	PAN	over HUSY
HCN (27)	2.04	5	10
Acetonitrile (41)	2.17	2	34
2-Propenenitrile (53)	2.19	8	15
Propanenitrile (54)	2.32	0.36	5
2-Methyl-2-propenenitrile (67)	2.35	2	4

molecular mass nitriles increased significantly, moreover numerous C4- and C5-nitrile isomers occurred while dimers and trimers were no longer detectable in the modified pyrolysate. Additionally several aromatic nitriles—mostly methyl- and dimethylbenzonitriles—and aromatic hydrocarbons formed as well.

In the case of ABS and SAN the pyrograms show that 2-propenenitrile, benzene, toluene, ethylbenzene, styrene and α-methylstyrene are still present, and the intensity of aromatic compounds is increased. Nevertheless, similarly as in the case of PAN pyrolysate dimers and trimers no longer occur after conversion. This effect can be explained by cracking and aromatization of the larger molecules while the smaller ones can pass through the zeolite channels without any change. Brownish colour of used NaY zeolite indicates that coke also deposited on it.

2.2.2 Conversion over HUSY. Table 1 shows those nitriles that still remain in the pyrolysis oil of PAN after being converted over HUSY. Although only aromatics are present besides these nitriles, the intensity of aromatic compounds is much less than in case of any other N-containing polymers. Presumably the decreased number of volatile compounds is the consequence of ladder structure formation and carbonization of the PAN chain fragments, leading more likely to carbon black than to aromatic hydrocarbon formation because HUSY promotes cyclization, dehydrogenation, aromatization, and crosslinking reactions.

Carbonization also explains the increased amount of HCN in the converted pyrolysate over HUSY.

The (c) chromatograms in Fig. 5–6 clearly show the strong aromatization effect of HUSY. All dimers and trimers of ABS are converted to benzene, naphthalene and their alkyl derivatives and even styrene disappears from the pyrograms.

Although both catalysts reduce the N-content of the pyrolysis oils, acetonitrile, 2-propenenitrile still remain and propanenitrile appears in the oil (Table 2). The intensity of acetonitrile increases, while the amount of 2-propenenitrile decreases over both catalysts, however changes are more spectacular over HUSY.

2.3 Pyrolysis product of polyurethanes

At 500 °C the decomposition of polyester based polyurethane (PUR_{est}) leads to the formation of CO_2, 1,3-butadiene, tetrahydrofuran (THF), cyclopentanone, bis(4-isocyanatophenyl)methane (MDI), and a number of ester compounds (Fig. 7a). In the pyrolysate of the studied polyether based polyurethane (PUR_{eth}) there are two major pyrolysis products, namely THF and MDI (Fig. 8a), and several ethers of low intensity.

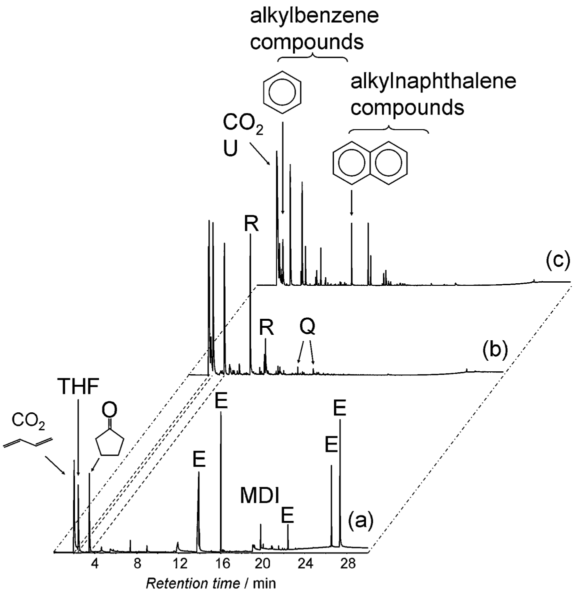

Fig. 7 Pyrolysis-gas chromatogram of PUR_{est} at 500 °C (a), the chromatogram of the pyrolysate converted over NaY (b) and over HUSY zeolite (c). E, ester compounds; MDI, bis(4-isocyanatophenyl)methane; Q, quinoline compounds; R, aromatic amines (especially aniline and alkylaniline compounds); THF, tetrahydrofuran; U, unsaturated and/or cyclic hydrocarbons.

2.3.1 Conversion over NaY. The (b) chromatograms of Fig. 7–8 are interpreted by the alteration of MDI and the ester/ether compounds of high molecular mass over NaY resulting in aromatic compounds while CO_2, 1,3-butadiene, THF, and cyclopentanone remain unchanged. Comparing the two chromatograms it can be seen that the peak heights of N-containing aromatic compounds are higher in case of PUR_{eth} than of PUR_{est}. Considering that the amount of MDI is much greater in the pyrolysate of PUR_{eth}, we may assume that aniline, quinoline and pyrrole compounds are derived from MDI, while aromatic hydrocarbons are formed by cracking of esters and ethers.

Table 2 GC-MS selected ion peak areas [(counts/mg polymer) ×10^{-7}] of small molecular mass nitriles in (a) and (c) chromatograms of *co*-polymers (Figs. 5 and 6)

			Catalyst			Catalyst	
Compounds and selected ions (m/z)	*Retention time*/min	ABS	NaY	HUSY	SAN	NaY	HUSY
Acetonitrile (41)	2.17	6	24	26	3	22	15
2-Propenenitrile (53)	2.19	76	43	13	48	34	9
Propanenitrile (54)	2.32	0	4	9	0	3	4

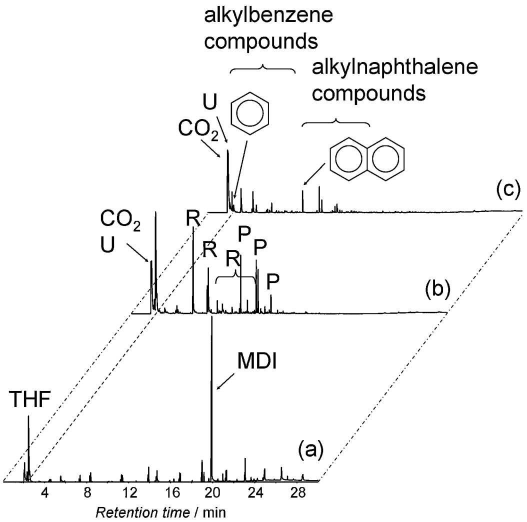

Fig. 8 Pyrolysis-gas chromatogram of PUR_{eth} at 500 °C (a), the chromatogram of the pyrolysate converted over NaY (b) and over HUSY zeolite (c). MDI, bis(4-isocyanatophenyl)methane; P, heterocyclic (N-containing) aromatic compounds; R, aromatic amines (especially aniline and alkylaniline compounds); THF, tetrahydrofuran; U, unsaturated and/or cyclic hydrocarbons.

2.3.2 Conversion over HUSY. The effect of HUSY is more characteristic than that of NaY demonstrated in Fig. 7–8. Alkylbenzene and alkylnaphthalene compounds are the major components of the converted pyrolysate; CO_2 and unsaturated/cyclic hydrocarbons of 3–6 carbon atoms are not altered.

2.4 Catalyst regeneration

Catalytic activity of the original, deactivated and regenerated zeolites has been tested by pyrolysis-gas chromatography/mass spectrometry (Py-GC/MS). The modification of PA-6,6 pyrolysis oil composition was studied over the original, deactivated and regenerated zeolites. We have found that the deactivated catalyst did not alter the pyrolysis oil composition, namely its activity has been lost. However, the catalytic effect of the regenerated zeolite becomes similar to that of the original one, that is its activity has been recovered.

Thermogravimetry-mass spectrometry (TG-MS) measurements in air provide information about the amount and quality of coke deposited on zeolite. The original and regenerated zeolites have similar TG, DTG and selected MS ion curves: mass loss of 6–8% is observed between 87–97 °C due to water desorption. Coke burn-off of deactivated zeolites occurs between 400–600 °C. In Fig. 9 TG, DTG and ion curves of deactivated zeolites are displayed. The coke burn-off was observed at 510 °C for deactivated NaY, and at 584 °C for deactivated HUSY, moreover, the corresponding mass loss was a few % higher from HUSY than from NaY. It must be mentioned that not only the temperature of coke burn-off but the DTG peak widths are also dissimilar for NaY and HUSY (shown in Fig. 9) that refers to differences in physical and chemical properties of the coke deposited on NaY and HUSY. Selected ion curves monitored in TG-MS at m/z 30 and 44—indicating the combustion products of nitrogen- and carbon-containing materials—have maxima at somewhat different temperatures, admittedly because the carbonaceous deposit is not homogenous either chemically or physically. MS ion at m/z 30 is attributed to NO, although it may refer to the presence of cyclic ethers and methoxy aromatics as well, but elemental analysis measurements clearly proved the increased nitrogen content in the deactivated zeolite samples (Table 3).

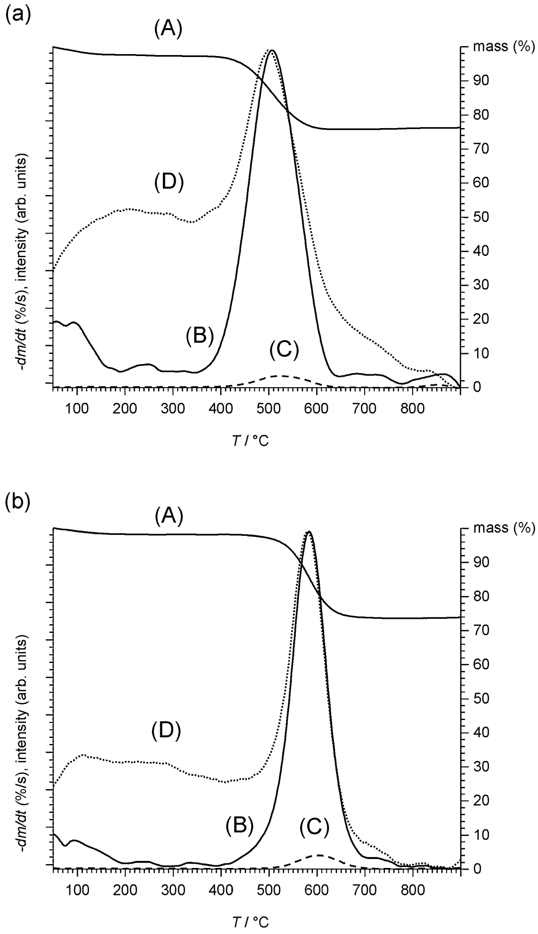

Fig. 9 Thermogravimetric analysis of deactivated NaY (a) and HUSY (b) zeolite. TG and DTG curves, full line (A) and (B), resp.; TG-MS ion profiles monitored for NO (m/z 30), dashed line (C); and for carbon dioxide (m/z 44), dotted line (D).

The crystal structure of original, deactivated and regenerated catalysts has been tested by comparing the characteristic XRD

Table 3 Nitrogen content and [3,5,5] XRD peak intensity of the zeolites

Catalysts	Elemental analysis	XRD
	N (wt%)	[3,5,5] peak intensity (counts)
original NaY	0.5	1050
once deactivated NaY	0.8	1369
once regenerated NaY	0.7	1069
thrice deactivated NaY	1.0	1305
thrice regenerated NaY	0.6	1050
original HUSY	0.4	1204
once deactivated HUSY	1.0	1082
once regenerated HUSY	0.8	882
twice deactivated HUSY	1.1	935
twice regenerated HUSY	0.5	797

Table 4 BET data of original, deactivated, thrice deactivated, regenerated and thrice regenerated NaY zeolites

	NaY	deactivated NaY	regenerated NaY	thrice deactivated NaY	thrice regenerated NaY
BET Area (m^2/g)	nc	11	nc	6	nc
Langmuir surface area (m^2/g)	1153			7	1053
Micro pore surface area (m^2/g)	1097	8	1484	7	997
Total pore volume (cm^3/g)[a]	0.433	0.046	0.620	0.033	0.405
Micro pore volume (cm^3/g)	0.391	0.003	0.529	0.002	0.355
Average pore width (nm)	0.67	2.88	0.84	2.69	0.71

[a] Calculated at $P/P_0 = 0.993$ nc: not countable (BET equation has no positive C solution.)

Table 5 BET data of original, deactivated, twice deactivated, regenerated and twice regenerated HUSY zeolites

	HUSY	deactivated HUSY	regenerated HUSY	twice deactivated HUSY	twice regenerated HUSY
BET Area (m^2/g)	nc	18	nc	7	nc
Micro pore surface area (m^2/g)	1016	18	908	8	838
Total pore volume (cm^3/g)[a]	0.438	0.088	0.435	0.029	0.378
Micro pore volume (cm^3/g)	0.362	0.006	0.324	0.003	0.299
Average pore width (nm)	0.95	2.56	1.03	2.56	0.95

[a] Calculated at $P/P_0 = 0.993$ nc: not countable (BET equation has no positive C solution.)

patterns. Peak intensity of [3,5,5] was observed in order to examine framework properties of the zeolites (Table 3). It does not decrease in the course of operation and regeneration of NaY zeolite, the intensities of the other peaks are changed only slightly in all cases indicating that the framework structure of NaY has not been damaged. Decreasing intensity of peak [3,5,5] after exploitation and regeneration of HUSY is explained by the vaguely changing framework properties. It is likely that coke has not been totally eliminated from HUSY by regeneration at 500 °C while coke deposited on NaY has been burned off. Note in TG experiments coke burn-off peak temperature of HUSY is around 70 °C higher than that of NaY.

BET measurements also revealed that catalysts regeneration were successful in the case of NaY. Table 4 shows that the values of micro pore surface area, total pore volume, micro pore volume and average pore width of the original and regenerated NaY zeolites are of the same order of magnitude, while the surface area and pore volume values of the deactivated NaY are significantly lower that those of the original zeolite. Somewhat decreased values of micro pore surface area, total pore volume, micro pore volume of regenerated HUSY zeolite (Table 5) indicate mild deactivation.

3.0 Experimental

3.1 Materials

3.1.1 Nitrogen-containing polymers. (a) polyamides: polyamide-6,6 (PA-6,6), polyamide-6 (PA-6) (BASF) and polyamide-12 (PA-12)

(b) *co*-polymers: poly(acrylonitrile-*co*-butadiene-*co*-styrene) (ABS), (with acrylonitrile of 25 wt.%) and poly(styrene-*co*-acrylonitrile) (SAN) (laboratory prepared), (with acrylonitrile of 19 wt%)

(c) polyacrylonitrile (PAN)

(d) polyurethanes: aromatic polyester based polyurethane (PUR_{est}) and polyether based polyurethane (PUR_{eth}) (BF Goodrich, Belgium)

Polymers without indicated source were used as received from Sigma-Aldrich and contained no additives.

3.1.2 Catalysts. Zeolites used in this study were Y zeolites with average pore diameter 0.74 nm, namely ultra stable hydrogen form of Si/Al = 2.49 (HUSY) and sodium form of Si/Al = 2.44 (NaY) (Grace Davison). The surface area and pore volume of zeolite catalysts are given in Tables 4–5.

3.2 Pyrolysis-gas chromatography/mass spectrometry (Py-GC/MS)

Pyrolysis-catalysis experiments were performed at 500 °C for 20 s in a Pyroprobe 2000 (Chemical Data System, USA) pyrolyser equipped with a platinum coil and quartz sample tube, coupled to Agilent 6890 GC-5973 MSD (Agilent Technologies, USA) instrument.

Two catalyst microbeds were placed at both ends of the sample holder quartz tube, making the pyrolysis vapour pass through the catalyst heated at the same temperature as the sample. Approximately 0.1–0.3 mg of the polymer sample was pyrolysed, the mass of the catalyst beds were 0.5–0.9 mg at both sides of the sample. Helium carrier gas at a flow rate of 20 mL min^{-1} purged the pyrolysis chamber held at 250 °C that was split prior to being introduced into the GC column.

The GC separation was performed on a HP-5MS capillary column (30 m × 0.25 mm × 0.25 μm) (Agilent Technologies, USA). After 1 min of isotherm period at 50 °C the oven temperature was programmed to 300 °C at 10 °C min^{-1} heating rate and held at 300 °C for 4 min. The temperature of the transfer line of GC/MS and the source of the mass spectrometer were 280 and 200 °C, respectively. The mass spectrometer was operating in electron-impact mode (EI) at 70 eV. The spectra were obtained over a mass range of 14–450 Da. The GC/MS identification of pyrolysis products has been carried out by using mass spectral library, mass spectrometric identification principles and gas chromatographic retention relations.

3.3 Thermogravimetry-mass spectrometry (TG-MS)

The TG-MS experiments were performed under oxidative atmosphere (argon with 21 (V/V)% oxygen) using a Perkin-Elmer TGS-2 thermobalance connected to a Hiden HAL/PIC mass spectrometer.

Before the experiments, the apparatus was purged with the carrier gas for one hour. The catalyst powder of about 0.5 mg was then heated at 10 °C min^{-1} up to 900 °C. The gas flow rate was 140 mL min^{-1} in all experiments.

A portion of the volatile products was introduced into the ion source of the mass spectrometer through a glass lined metal capillary held at 300 °C. The quadrupole mass spectrometer was operated in electron impact ionization mode with 70 eV electron energy. The ion intensities were normalised to the sample mass and to the intensity of the ^{38}Ar isotope of the carrier gas.

3.4 Elemental analysis

Nitrogen and oxygen contents of the original, deactivated and regenerated catalysts were measured using HORIBA EMGA-620W-Oxygen/Nitrogen Combustion Analyzer.

3.5 X-ray diffraction (XRD)

X-ray diffraction (XRD) patterns of the original, deactivated and regenerated zeolites were recorded by a Philips PW1810/1870 diffractometer using monocromatized Cu-K$_\alpha$ radiation (40kV, 35 mA). The XRD scans were digitally recorded with a step-size of $2\theta = 0.02°$.

3.6 BET surface area measurements

Specific surface area, micro pore volume, micro pore surface area and total pore volume of the original, deactivated and regenerated catalysts were determined by nitrogen adsorption at −196 °C by a Quantachrome Autosorb-1-C gas sorption analyser. Dubinin-Radushkevich (DR) method was applied to micro pore analysis.

3.7 Catalysts deactivation and regeneration

Catalysts' deactivation was carried out at 500 °C in N_2 flow (20 mL min^{-1}) for 30 minutes in a Carbolite MTF 12/38/250 furnace. As Fig. 10 shows the catalyst bed was placed behind the quartz sample holder, thus the N_2 flow carried the pyrolysis vapour through the bed.

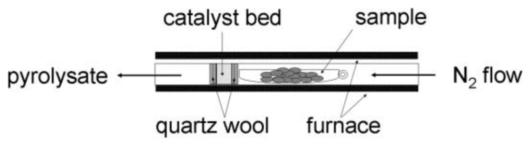

Fig. 10 Schematic illustration of sample arrangement in the furnace for studying catalysts' coking behaviour.

The mass of the catalyst bed was 3 g and approximately 9 g polymer mixture was pyrolysed, in which PA-6,6, ABS and PUR were mixed in equal proportion. This ratio of catalyst and polymers was appropriate for complete deactivation of the catalysts.

After the polymer char removal the catalyst bed was also taken out and the catalyst was separated from the quartz wool. Then the catalyst was divided into two. One portion was put in a plastic vessel as a reference for further measurements; the other portion was placed into the furnace in a quartz sample holder. The regeneration was performed at 500 °C in air flow (20 mL min^{-1}) for 8 hours.

Once and twice deactivated and regenerated HUSY while once and thrice deactivated and regenerated NaY have been tested.

4.0 Conclusion

Pyrolysis and regeneration studies revealed that both NaY and HUSY zeolites can be used and reused under 500 °C pyrolysis conditions to reduce the nitrogen content of the pyrolysis oil of N-containing polymers. The catalysts efficiently transform the pyrolysis oils into a mixture that dominantly contains olefins and aromatics of low molecular mass. Although both zeolites open up new prospects in N-containing polymer recycling through the conversion of pyrolysis oil, there are characteristic differences in the composition of the modified oils as follows:

Over NaY zeolite

- The modified pyrolysate contains low molecular mass compounds only and its composition is strongly related to the components of the original pyrolysis oil.
- Low molecular mass N-containing thermal decomposition products of polymers are still present invariably in the converted pyrolysate, while long chain amides, amines, nitriles and diisocyanate are converted into N-containing aromatic, alkylaromatic and cyclic compounds.

Over HUSY zeolite

- The modified pyrolysis oils derived from different polymers have common characteristics.
- The main compounds of modified pyrolysate are low molecular mass olefins and aromatics dominantly alkylbenzene and alkylnaphthalene compounds in all cases except PAN.
- The only N-containing compounds detected in the converted pyrolysates are nitriles in the range of 1–8 carbon atoms; their amount rapidly decreases with increasing molecular mass.

The framework structure of zeolites is not damaged at the temperature of operation of pyrolysate conversion and the catalytic activity decreased due to coke deposit can be recovered by thermal treatment in air.

Acknowledgements

The authors are grateful to Emma Jakab and Zoltán Sebestyén for their kind help in TG-MS measurements, Zoltán Károly for BET measurements, Cecilia Bartha for elemental analysis, Ágnes Szegedi for XRD measurements. This work was supported by the Hungarian National Research Fund (OTKA) contract no. K68752.

Notes and references

1 J. Scheirs, and W. Kaminsky, (Eds.), (*Feedstock Recycling and Pyrolysis of Waste Plastics*, Wiley, Chichester, 2006.
2 M. Blazsó, G. Várhegyi and E. Jakab, *J. Anal. Appl. Pyrolysis*, 1980, **2**, 177.
3 H. Ohtani, T. Nagaya, Y. Sugimura and S. Tsuge, *J. Anal. Appl. Pyrolysis*, 1982, **4**, 117.
4 Ballistreri, D. Garozzo, M. Giuffrida and G. Montaudo, *Macromolecules*, 1987, **20**, 2991.
5 M. Herrera, M. Wilhelm, G. Matuschek and A. Kettrup, *J. Anal. Appl. Pyrolysis*, 2001, **58–59**, 173.
6 W. J. Hall and P. T. Williams, *J. Anal. Appl. Pyrolysis*, 2006, **77**, 75.
7 S. Czernik, C. C. Elam, R. J. Evans, R. R. Meglen, L. Moens and K. Tatsumoto, *J. Anal. Appl. Pyrolysis*, 1998, **46**, 51.
8 Z. Sarbak and M. Lewandowski, *Appl. Catal., A*, 2001, **208**, 317.
9 D. Ferdous, A. K. Dalai and J. Adjaye, *Appl. Catal., A*, 2004, **260**, 137.
10 T. Bhaskar, K. Murai, M. Brebu, T. Matsui, Md. A. Uddin, A. Muto and Y. Sakata, *Green Chem.*, 2002, **4**, 603.
11 C. Vasile, H. Pakdel, M. Brebu, P. Onu, H. Darie and S. Ciocalteu, *J. Anal. Appl. Pyrolysis*, 2001, **57**, 287.
12 M. Blazsó, *J. Anal. Appl. Pyrolysis*, 2005, **74**, 344.
13 W. J. Hall and P. T. Williams, *J. Anal. Appl. Pyrolysis*, 2008, **81**, 139.
14 H. G. Karge, in *Studies in Surface Science and Catalysis: Introduction to Zeolite Science and Practise*, ed. H. van Bekkum, E. M. Flanigen, and J. C. Jansen, Elsevier, Amsterdam, 1991, vol. 58, ch. 14, pp. 531-570.
15 V. Babich, K. Seshan and L. Lefferts, *Appl. Catal., B*, 2005, **59**, 205.
16 Marcilla, M. I. Beltrán and R. Navarro, *J. Anal. Appl. Pyrolysis*, 2005, **74**, 361.
17 J. Bozi, Zs. Czégény and M. Blazsó, *Thermochim. Acta*, 2008, **472**, 84.